Received 15 December 2015
Revised 9 May 2016
Accepted 24 June 2016

Mission architecture for Mars exploration based on small satellites and planetary drones

Pierpaolo Pergola and Vittorio Cipolla
Department of Civil and Industrial Engineering – Aerospace Section, University of Pisa, Pisa, Italy

Abstract

Purpose – The purpose of this paper is to deal with the study of an innovative unmanned mission to Mars, which is aimed at acquiring a great amount of detailed data related to both Mars' atmosphere and surface.
Design/methodology/approach – The Mars surface exploration is conceived by means of a fleet of drones flying among a set of reference points (acting also as entry capsules and charging stations) on the surface. The three key enabling technologies of the proposed mission are the use of small satellites (used in constellation with a minimum of three), the use of electric propulsion systems for the interplanetary transfer (to reduce the propellant mass fraction) and lightweight, efficient, drones designed to operate in the harsh Mars environment and with its tiny atmosphere.
Findings – The low-thrust Earth-Mars transfer is designed by means of an optimization approach resulting in a duration of slightly more than 27 months with a propellant amount of about 125 kg, which is compatible with the choice of considering a 500 kg-class spacecraft. Four candidate drone configurations have been selected as the result of a sensitivity analysis. Flight endurance, weight and drone size have been considered as the driving design parameters for the selection of the final configuration, which is characterized by six rotors, a total mass of about 6.5 kg and a flight endurance of 28 minutes. In the mission scenario proposed, the drone is assumed to be delivered on the Mars surface by means of a passive entry capsule, which acts also as a docking station and charging base. Such a capsule has been sized both in terms of mass (68 kg) and power (80 W), showing to be compatible with 500 kg-class spacecraft.
Research limitations/implications – As a general conclusion, the study shows the mission concept feasibility.
Practical implications – The concept would return incomparable scientific data and can be also be potentially implemented with a relatively low budget exploiting of the shelf components to the larger extent, small identical spacecraft buses and modular low-cost drones.
Originality/value – The innovative mission architecture proposed in this study aims at providing a complete coverage of the surface and lowest atmospheric layers. The main innovation factor of the proposed mission consists in the adoption of small multi-copter UAVs, also called "drones," as remote-sensing platforms.

Keywords UAVs, Electric propulsion, Mars, Planetary drones, Small satellites
Paper type Research paper

1. Introduction

Besides the regions explored so far by the planetary rovers in the framework of the Viking, MSR, Pathfinder and Curiosity programs (McCleese), Mars presents several unexplored regions of high potential interest. The boundary between heavily cratered southern highlands and the smooth northern lowlands, for instance, shows some structures resulting by water/ice erosion. The Cydonia Mensae (Guest *et al.*, 1977), a mesa-like structure, observed only by the Viking 1 and Mars Express, is thought to have hosted ancient seas or lakes. These were later covered by lava and sediment deposits, but only a close look at this region can confirm this and the subsequent water erosion that left the debris-filled valleys detected by orbital images. In the region there

International Journal of Intelligent Unmanned Systems
Vol. 4 No. 3, 2016
pp. 142-162

2049-6427
DOI 10.1108/IJIUS-12-2015-0014

are several impact craters where the material inside the walls seems to have been slumped away from the rim or with smooth floors with raised rims and rounded rings of ejecta around them, thus suggesting that the impacts were into an ice- or water-saturated terrain. In this region there are mounds of debris with a different surface texture and a higher density of impact craters. This might be the proof that they belonged to the older southern highlands area and they have been brought there by water/ice movements. Once more these are speculations based on images from satellites and/or direct exploration of nearby regions.

Due to the nature of the Cydonia Mensae (takes as an example of the many interesting regions on Mars not yet sufficiently explored), a rover might not reveal the details we are looking for. Valleys, debris, craters and so on make this region particularly hard to explore if not by orbital altitudes, but at the same time the regions more difficult to study, such as the transition ones, are the most rich in terms of clues to understand the nature and the evolution of the planet.

The Mars surface exploration aimed at searching for signs of past water activity, surface rock composition, chemically induced geological processes, amount of iron-containing materials and the general surface texture. The paper presents a possible solution for a wide coverage of the Mars surface at few tens of meters height. Arduous regions (but not only) can be explored by means of a fleet of multirotor unmanned aerial vehicles, hereafter called drones, equipped with different payloads. To achieve this goal the mission architecture presented includes also a set of surface stations, allowing drones to land safely and recharge, working as reference points for the autonomous navigation system and acting as data transponders toward the orbiting probe.

In the next sections the overall mission architecture is presented. Section 3 details the Earth-Mars low-thrust transfer and in Section 4 preliminary spacecraft sizing is given. The drone design approach is presented in Sections 5 and 6 show the resulting drone design and sizing. Finally, Section 7 deals with the design of entry capsules and docking stations.

2. Mission architecture and Mars surface science phase

The mission architecture here proposed is based on the idea that a drone can carry out both surface coverage and atmospheric mapping wider than any rover or lander module. To implement this approach, however, several technical and conceptual issues have to be faced. First of all, the drones have to be sized to survive the harsh Mars weather conditions. In this study this aspect is taken into account by designing a drone specifically sized on the Mars atmospheric characteristics and by using to the larger extent off-the-shelf components (in particular batteries and motors) already designed and possibly flown in space.

After the interplanetary transfer, the drone is supposed to be brought on Mars surface by means of a passive entry capsule (Edquist *et al.*, 2008), which is released by the mother spacecraft which remains in orbit. Once on the surface, the drones must be able to rely on an autonomous navigation system. This is one of the main issues that the mission architecture proposed aims at solving by means of a multi-mission approach. Indeed the mission is composed of a minimum of three identical probes. Each probe has as payload the same entry capsule (acting also as a docking station for the drone on the Mars surface) equipped with a single drone. In this way, the fleet can rely on a minimum set of three reference points. In this perspective, it has been also chosen to limit the probe mass to 500 kg and to equip each one with an autonomous propulsion system without relying on hyperbolic excess velocity. This allows both

multiple launches with medium-size launchers and a single launch with multiple payloads (of a total of 1,500 kg). This approach has been preferred to a single heavy probe because of the lower development and production cost of a small satellite and the intrinsic redundancy it offers. Moreover, this configuration takes advantage from the mass series production, where additional identical satellites can be launched in the future to increase the Mars surface coverage without further non-recurring costs.

The concept here proposed offers several unique advantages with respect to common planetary exploration approaches. The use of a fleet of small satellites enables more affordable missions whereas electric propulsion allows for an increased payload mass fraction. Dealing with the surface exploration concept, the deployment of drones allows to explore also the most arduous regions, often not even accessible to surface rovers, with lower loitering speed and hovering capabilities, that cannot be achieved by means of fixed-wing planes. Figure 1 provides an overview of the concept of operations proposed.

Mars surface operations are carried out by a fleet of at least three drones, which are required to have a sufficient set of reference points for the autonomous navigation system (Maimone *et al.*, 2006). Additional launches can be considered without changing the overall mission architecture. Drones can fly among the docking stations and, once one mission is completed, they can recharge by docking on one of those. Drone autonomy is the main factor constraining the area covered. In the study drones have been designed aiming to achieve an endurance of 30 minutes.

The drone payload is composed of electro-optical sensors for the surface explorations and probes for the atmospheric scan (although different payloads can be conceived for the forthcoming drones). The drones are designed to rely on their battery energy to operate the motors, to run the on-board computer and the payload. Data acquired by the payload are stored on-board and downloaded to the docking station at the end of each mission. The docking station is thus also in charge of uplinking these data to the orbiting spacecraft acting as data relay toward the Earth. The docking station is integrated into the landing capsule that, once on the surface, acts as reference point for the navigation system, as docking station to recharge drones and as transponder to the probe. During the touchdown phase the backshell is separated from the landing capsule together with the parachute. Since it is assumed to fly away from the capsule, the backshell is also equipped with a small beacon in order to act as an additional reference point for the navigation system.

3. Earth-Mars low-thrust transfer

In order to limit the overall mission cost, it has been chosen to consider a spacecraft size at the limit between small and medium class satellites. A 500 kg spacecraft is

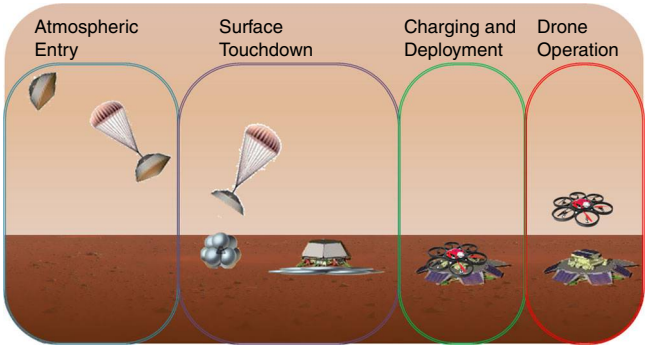

Figure 1.
Mission concept of operations

considered to be placed on an Earth escape trajectory with zero hyperbolic excess velocity, assumption compatible with the great majority of medium class launcher (e.g. Atlas V and Delta II). The spacecraft size is not unrealistic for interplanetary missions, as a comparison the Mars Odyssey spacecraft mass is about 730 kg (Mars Odyssey Arrival Press Kit, 2001), New Horizon weighs about 478 kg (New Horizons Launch Press Kit, 2006) and Deep Space 1 about 490 kg (Deep Space 1 Press Kit, 1998).

With the general aim of reducing the propellant mass fraction, thus increasing the payload that can be delivered into the target orbit around Mars, the spacecraft is assumed to be equipped with an electric propulsion system. Due to the intrinsic nature of such a kind of propulsion, indeed, the propellant is expelled with a high exhaust velocity, which means high-specific impulse, thus the amount of propellant required to complete a given mission is smaller than a classical chemical thruster. On the other side, such a kind of propulsion delivers a lower thrust magnitude so it has to be operated for extended trajectory arcs to reach the mission total impulse.

The Earth-Mars transfer trajectory is designed by considering the dynamics of the probe under the Sun gravitational influence and the thruster acceleration. Once the probe reaches the Martian sphere of influence, the capture trajectory, which goes from the sphere of influence to the target orbit around the planet, accounts for Mars as the main attractor whereas the Sun and the electric thruster act as perturbations.

Trajectory is designed in the heliocentric three-dimensional reference frame with non-dimensional units and equations of motion are integrated with the Runge-Kutta 4-5 scheme with absolute and relative tolerance of 1e-11.

The mission conceived is unmanned thus, in line with the philosophy of using an electric propulsion system, the final probe mass is maximized, rather than the transfer time. The indirect Pontryagin's minimum principle (Bryson and Ho, 1975) is used to define the optimal thrust laws for the minimum mass problem. Lagrange multipliers rule the thrust direction, defining the in-plane and out-of-plane thrust angles. During the transfer, the thruster can be also switched off (minimum mass transfer in a fixed time) according to the behavior of a switch function also ruled by the Lagrange multipliers. The thruster power level is decreased with the inverse square law with the heliocentric distance.

The heliocentric transfer ends at the boundary of the Mars sphere of influence. Afterwards a low-thrust spiraling-down procedure is implemented following some standard thrust directions. In particular: thrust is implemented when the specific mechanical energy with respect to Mars is lower than 0, i.e. the probe is (even temporarily) captured by the planet gravity field; anti-tangential thrust is considered until the orbital apocenter is larger than the target value, in this case thrust is applied in an arc between $\pi/4$ and $7\pi/4$ around the pericenter to reduce the orbital eccentricity as well; in case the periradius is smaller than the target value, the thrust is directed perpendicular to the radius vector to speed up the spacecraft avoiding it to enter the Martian atmosphere and burn up.

The spacecraft is supposed to be equipped with a NSTAR electric thruster (Sovey *et al.*, 2001) operated with xenon at nominal conditions. It requires an input power of 2,300 W to deliver 92 mN thrust with 3,100 s of specific impulse. At Mars the same thruster is run with 1,120 W delivering about 45 mN. It has been arbitrarily assumed to limit the interplanetary transfer time at 18 months. Accordingly, a set of minimum mass transfers have been designed with a transfer duration of between 518 (minimum time transfer) and 540 days.

Figure 2 shows the heliocentric transfer with indication of the thrust direction (left) and the Mars capture phase inside the Mars sphere of influence (right) for the 530 days transfer.

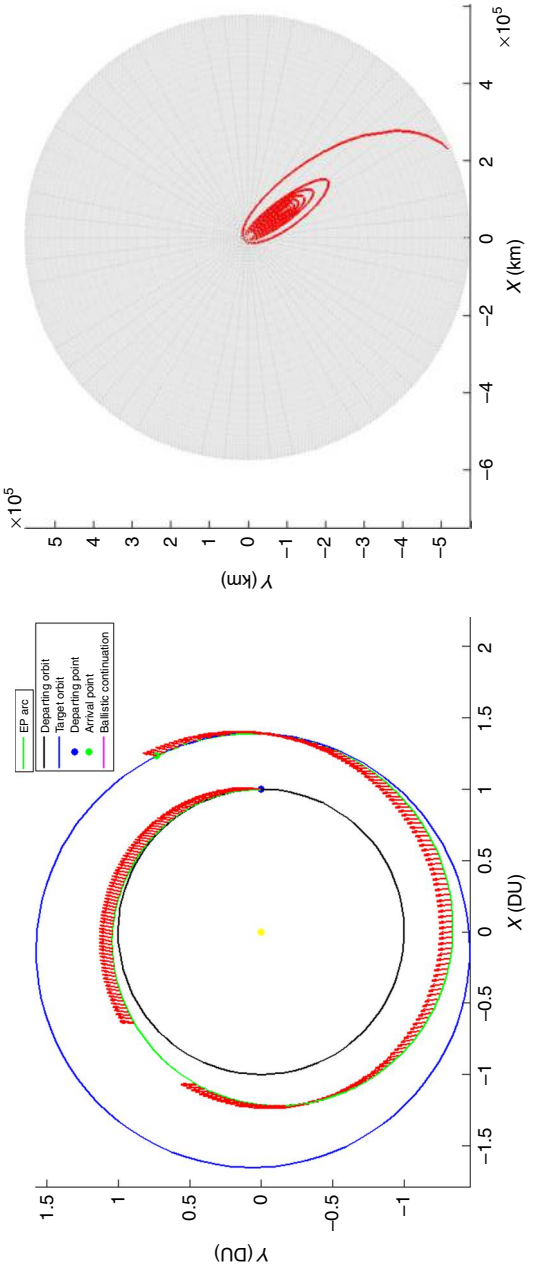

Figure 2.
Interplanetary low-thrust transfer (left) and detail of the low-thrust capture phase insider the Mars sphere of influence

This option offers the best compromise, in the range investigated, between transfer time and mass consumption; thus it has been considered as baseline solution. A 540 days transfer, indeed would save less than 2 kg of propellant, while the minimum time transfer requires 518 days and 91.7 kg of xenon (in this case no coasting arc takes place). In any case, the mission conceived requires only minor changes considering other reference solutions; i.e. few kilograms in the final mass and/or few weeks shorter/longer transfer time.

The first phase of the heliocentric transfer requires about 32.4 kg of propellant and 130 days, it is used to increase the orbital energy and spiraling out from Earth's orbit. Afterwards a coasting phase of 37 days takes place (duration determined by the optimization scheme), which is followed by another thrusting phase of 363 days that with about 54.5 kg of propellant slows down the probe and circularizes the orbit preparing the following Mars capture. The resulting mission total velocity change (Dv) is 5.80 km/s (6.16 km/s for the minimum time solution). Figure 3 shows the time evolution of spacecraft position and velocity together with the in-plane and out-of-plane thrust angles, thruster input power and thrust level. The gray shadowed regions identify the coasting arc.

The parameters of the target areocentric orbit have been chosen according to reference Mars missions. Mars Global Surveyor, for instance, reached a target orbit around Mars with 175 km pericenter and 17,850 km apocenter (Albee *et al.*, 2001). Taking these data as reference, the capture phase lasts about 297.2 days and requires about 37.9 kg of xenon. The target orbit is characterized by an eccentricity of about 0.7115. The specific orientation of the orbital plane around Mars is not considered in the present analysis since a proper selection of the launch date and minimal orbital correction maneuverss can be implemented in the actual mission to target-specific conditions. During this phase the probe is already captured by the Mars gravity and the actual mission phase can start also during the spiraling down before achieving the final target orbit. Figure 4 shows the time evolution of the main orbital parameters and the specific mechanical energy of the probe with respect to Mars during the capture phase.

All in all, the complete transfer from Earth launch until the capture into the target orbit takes 827.2 days (about 300 days spent inside the Mars sphere of influence) and requires about 124.8 kg of propellant. Figure 5 shows the mass evolution during the heliocentric phase and the capture maneuver. The solid blue line represents the two heliocentric thrusting arcs (with non-constant propellant mass consumption due to the non-constant working point of the thruster), whereas the orange line refers to the coasting intermediate phase; the dashed magenta line, finally, shows the mass consumption during Mars capture.

4. Top-level spacecraft sizing

The spacecraft preliminary mass budget has been defined by considering some statistical reference figures of the main subsystems of interplanetary probes (Wertz *et al.*, 2011). A detailed design of each subsystem is left to further studies, but the preliminary mass assessment shows that a 500 kg-class spacecraft is sufficient to perform the proposed mission (see Table I).

The spacecraft preliminary power budget has been defined by considering the worst conditions, i.e. the concluding capture phase when the probe is around Mars and when the electric propulsion system is operated. In these conditions, the thruster requires 1,120 W and, assuming 90 percent efficiency of the power processing unit, 1,230 W has to be supplied by the electric propulsion system. The power required for other subsystems is estimated by means of reference figures valid for interplanetary probes

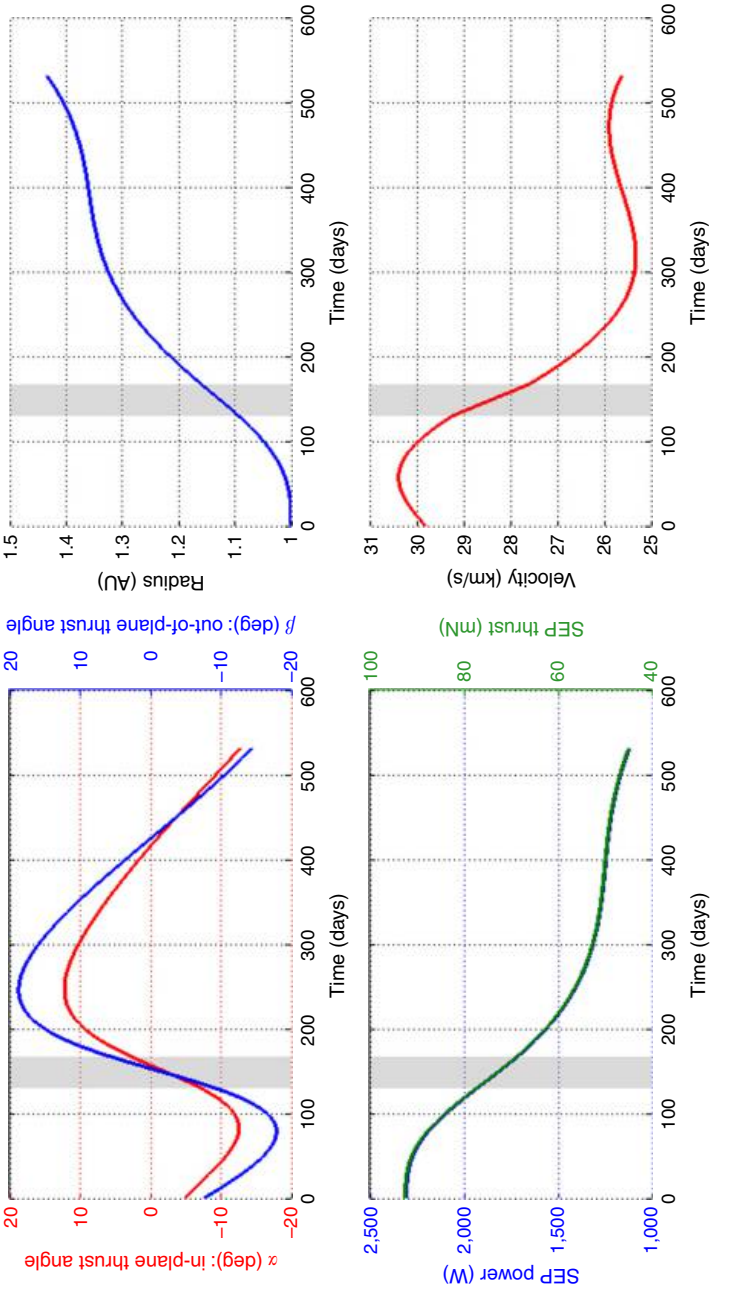

Figure 3.
From the upper left corner in clockwise direction: in-plane and out-of-plane thrust angles during the interplanetary transfer, time evolution of the probe heliocentric distance and velocity, power available for the electric propulsion system and thrust magnitude generated accordingly

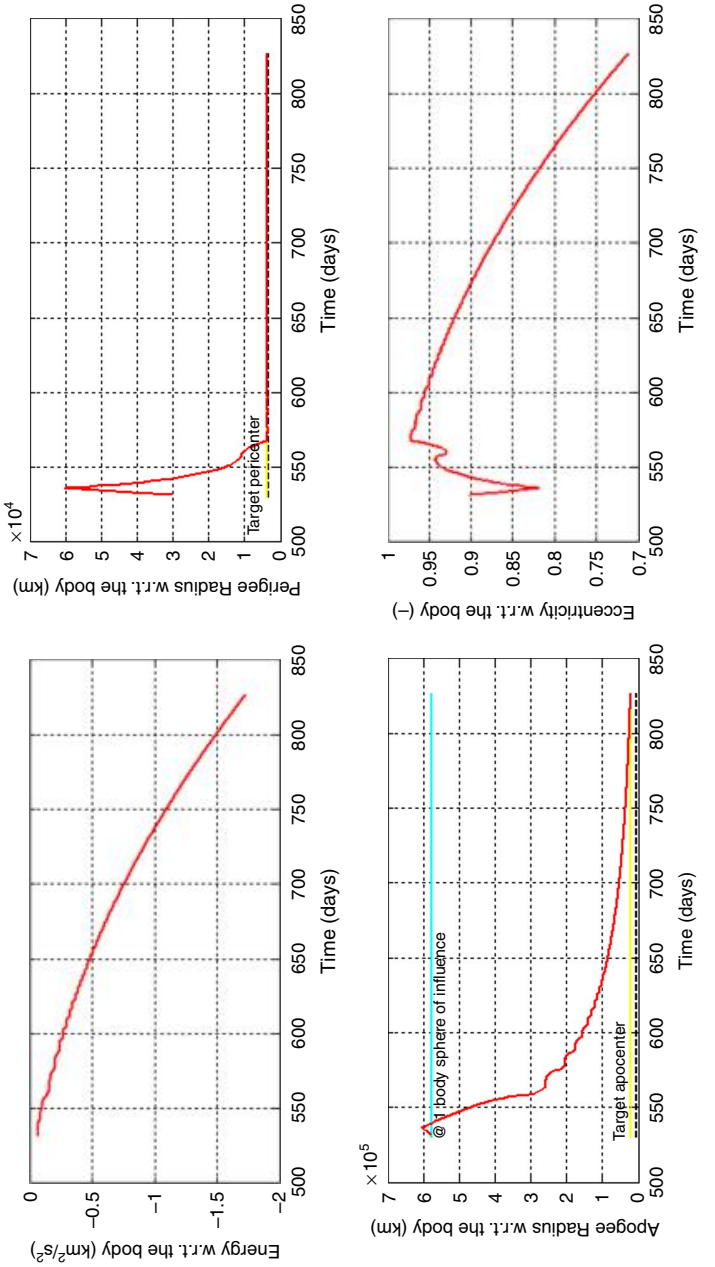

Figure 4.
From the upper left corner in clockwise direction the time evolution of relevant parameters during the Mars capture: specific energy, perigee radius, eccentricity and apogee radius

(Wertz *et al.*, 2011). This means that the power requirement in this condition is approximated by: $P_{TOT} = xP_{TOT} + P_{SEP}$, where x includes the percentage reference figures (see Table I). It results that about 3,850 W are required when firing during Mars capture; 4 kW are actually considered to take into account a system-level margin.

Assuming a 25 percent efficiency for solar arrays during the interplanetary transfer and accounting also for the solar panel degradation during the transfer, it results that about 27.3 m^2 of solar panels are required. On Earth, where solar array efficiency is assumed to be 28 percent, such surface generates about 10.4 kW. This allows for a significant power margin in the early mission phases (when the electric propulsion system requires 2,530 W), although this increased power level means a higher consumption for the power generation system and for the thermal control system. Indeed, it might be also possible to limit the incoming power via the on-board power management system and/or deploying part of solar arrays during the Earth-Mars path.

During the operative orbit, instead, the thruster is not continuously operated and the power surplus is used by the telecommunication and ADCS for ensuring the proper

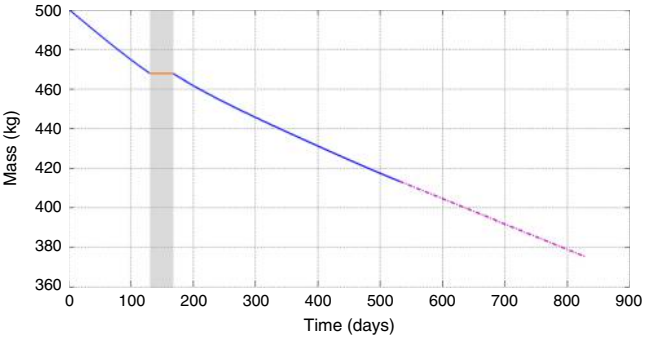

Note: The shadowed strip identifies the coasting arc (orange line)

Figure 5.
Time evolution of the spacecraft mass during the interplanetary phase (blue solid line) and during the Mars capture phase (magenta dashed line)

	Mass		Power budget in firing mode @ Mars		Power budget in firing mode @ Earth		Power budget in the target orbit	
Subsystem	Kg	% Tot	W	% Tot	W	% Tot	W	% Tot
Structure and mechanism	88	17.6	40	1.0	40	0.4	40	1.0
Thermal	21	4.2	600	15.0	1,000	9.6	600	15.0
Power generation	74	14.8	400	10.0	1,000	9.6	400	10.0
TT&C	25	5.0	720	18.0	720	6.9	1,000	25.0
OBDH	14	2.8	440	11.0	440	4.2	440	11.0
ADCS	21	4.2	480	12.0	480	4.6	1,000	25.0
Propulsion	46	9.2	1,230	30.8	2,530	24.3	20	0.5
Propellant	125	25.0 (*)	–	–	–	–	–	–
Total w/o payload	414	82.8	3,910	97.8	6,210	59.7	3,500	87.5
Payload	80	16.0 (*)	40	1.0	40	0.4	0	0.0
System-level margin	6	1.2	50	1.3	4,150	39.9	500	12.5
Total	500	100.0	4,000	100.0	10,400	100.0	4,000	100.0

Note: (*) of wet mass

Table I.
Spacecraft preliminary mass and power budget

attitude and the telecommunication both with the Martian lander and with the Earth ground station. These considerations are summarized in Table I.

It is worth mentioning that the power level identified is coherent with the preliminary mass budget. It results, indeed, in a power density of 150 W/kg (or even less), typical value for honeycomb substrate solar panels with multijunction solar cells (Law *et al.*, 2006). The NSTAR propulsion system, flown on-board of Deep Space 1 weighed 48 kg, in line with the preliminary mass estimation of Table I. The system includes, beside the thruster, the power processing unit, the xenon fluidic system and tank, the digital control and interface unit, cabling and harness (Brophy *et al.*, 2000). The propulsion subsystem consists of a single thruster firing for the whole mission duration: the NSTAR thruster is designed for a throughput of 150 kg, thus the mission is close to the limit of the thruster lifetime. To increase the contingency margin, a second thruster can be also considered in the probe design as cold redundancy, which adds approximately 8 kg of thruster, mechanical support and fluidic to the mass budget.

5. Planetary drone design approach

The drone is the actual mission payload. Such a platform offers wider surface exploration options, according to the specific sensor package considered; for instance it might allow for the acquisition of a 3D model of the Mars surface as well as for a complete atmospheric data collection.

In the past, different exploration aircraft, such as Wichita State University "MAEV" (Malla, 2000), NASA "ARES" (Braun and Spencer, 2006), NASA "ERAST" (Goebel, 2010) and StarTiger Dropter (Lutz *et al.*, 2014), have been proposed for the same purposes. Other relevant concepts worth mentioning are the Mars Airborne Geophysical Explorer, Airplane for Mars Exploration, Mars Advanced Technology Airplane for Deployment, Operations and Recovery, Advanced Reconnaissance Martian Deployable Aircraft, Martial Aerial Research Euroavia Airplane (Hall and Parks, 1998; Clapp, 1984; Development Sciences Incorporated, 1978).

Fixed-wing vehicles are very efficient on the aerodynamic side but require to fly at significantly high speed (50-70 m/s), which may affect the quality and the detail level of observations. A multi-copter drone, instead, allows for hovering, altitude changes, fast return missions on the most interesting points and so on; unique features making such a concept more appealing than a fixed-wing platform. The size and mass expected, moreover, can make such a concept more compact and flexible, thus more compatible with small spacecraft and light launchers.

The main components of the multi-copter are: the airframe, a set of propellers driven by brushless motors, an Li-ion battery pack, a flight controller system which includes the autopilot, an inertial measurement unit, and a communication and navigation module, which allows the drone to communicate with the docking stations to detect its position and perform the planned missions. The specific payload can be tailored and is different from drone to drone; in general the payload pack may consist in visible, infrared and/or multispectral camera, some air data and radiation sensors, meteorological air and wind sensors, pressure tubes, near-field magnetic target, X-ray spectrometers and so on.

As reference state of the art for payloads fitting within the mass and power constrains imposed (see Section 6), the APXS instrument can be considered. It is an α particle X-ray spectrometer used in Mars Pathfinder mission (Girones-Lopez *et al.*, 2010) and also flown on-board the comet lander Philae. Another valuable reference payload is a stereo camera system like the one used by the Beagle 2 mission

(Pullan *et al.*, 2004). Such a system consists of two cameras with different angles (suitable for 3D imaging) with a total mass of less than 350 g and about 1 W maximum power requirement.

The drone design approach has been first focused on the particularly challenging aerodynamic conditions propulsion systems have to face on Mars. In fact, the Mars atmosphere (Justus *et al.*), which is composed of carbon dioxide (95 percent), nitrogen (3 percent) and argon (1.6 percent), has a very low density (about 1 percent of Earth value at sea level) and, given the same speed conditions, Re numbers are about 0.5 percent of that of the Earth. In addition, Mars weather is characterized by average temperatures ranging between −5°C and −80°C (Rover Environmental Monitoring Station) and by a maximum wind speed of 30 m/s, which in terms of dynamic pressure is equivalent to a wind speed on Earth as low as 3 m/s.

Because of such atmospheric characteristics, propellers efficiency and motor reliability are the main issues of the design of a multi-rotor capable to fly on Mars. High-speed brushless motors for Martian applications have been already studied; e.g. in Phillips *et al.* (2012) where laboratory tests have been performed on a 22 mm diameter brushless DC motor, simulating the characteristics of Mars atmosphere. Results have shown that such motor can properly work at rotation speeds of up to 12,000 rpm and temperatures between −55°C and +40°C. As a consequence, in this study an upper limit of 11,000 rpm has been conservatively assumed to assess the feasibility of the design solutions investigated.

Concerning propellers, since a large part of the drone mission time is spent in hovering condition, ducted propellers can be used to save about 25-30 percent of power providing the same static thrust (Kuchemann and Weber, 1953; Helmbold, 1955). Ducted propellers have been designed by using the Ducted Fan Design Code (DFDC) developed at MIT, chosen for its low-computation cost and high flexibility. In DFDC, propeller blades are represented through the lifting-line model, whereas the duct and the center body are represented by axisymmetric panels (Drela and Youngren, 2005). Forces and moments given by blade sections are computed through the blade element theory and induced velocities are calculated taking the effects of the duct and center body on the flow field into account.

Atmospheric data, such as density (ρ), sound speed (a) and dynamic viscosity (μ), are the specific inputs allowing to simulate the Mars atmosphere. In particular, the following data have been used:

- $\rho = 0.015\ \text{kg/m}^3$;
- $a = 200\ \text{m/s}$; and
- $\mu = 1.08 \times 10^{-5}\ \text{kg/m s}$.

DFDC has been implemented into a numerical code allowing to manage the main propeller design parameters; in particular:

- duct internal diameter, D;
- number of blades, N;
- blades pitch angle, θ;
- mean geometric chord of the blade, c; and
- blade taper ratio (root chord/tip chord), λ.

The propeller design has been performed to both fulfill the vertical equilibrium between weight and thrust (plus a 10 percent margin for maneuverability) and obtain

an endurance of around 30 minutes. Thrust provided by the ducted propeller has been evaluated in static conditions, i.e. zero upstream velocity, assuming a reference twist angle distribution for the blades and a reference geometry for the duct and the center body.

As already mentioned, in order to guarantee BLDC motors reliability, rotation speed has been limited to 11,000 rpm. In addition, for each diameter considered the maximum rotation speed has been defined by applying an upper limit of 0.80 to the maximum local Mach number, reached at blade tips, in order to avoid shock waves.

A sensitivity analysis has been performed to evaluate the effects of the aforementioned parameters on the power-to-thrust ratio (P/T) and rotating speed-to-thrust ratio (n/T) in static conditions. The main results, shown in Figures 6 and 7, indicate that duct diameter, number of blades and mean blade chord are the most significant parameters ruling the drone design.

Figure 6 shows that for the same rotating speed value, P/T is lower for propellers with smaller diameters, lower number of blades and smaller chords, which is the obvious consequence of the aerodynamic drag generated by propeller blades. Since the thrust-weight balance requirement is met by calculating the actual rotating speed value for the propeller considered, the choice of "low drag" propellers leads to high rotating speed values which can cause shock waves on blades' tip and overheating problems to motors. Therefore, the sensitivity of the n/T ratio to the same set of parameters has been investigated (Figure 7), finding the opposite behavior.

Since a good propeller performance can be obtained if both P/T and n/T ratios have low values, it is necessary to find a good compromise for the set of design parameters (D, N, c). A group of possible solutions has been selected by using the chart shown in Figure 8, in which configurations between "sol#6" and "sol#14" have been indicated as the most promising candidates. The main characteristics of these two limit solutions are summarized in Table II.

Starting from the propeller performance, the drone has been designed by assuming a modular structure for the airframe. Each module consists of a propeller, a brushless motor and an annular element which acts both as duct and structural elements (see Figure 9).

6. Planetary drone preliminary sizing and design

The drone has been sized by taking the following top-level requirements into account:

- mass of sensors (drone's payload) = 0.7 kg;
- desired flight endurance of 30 minutes in hovering condition;
- static thrust must balance the weight increase of 10 percent for maneuvering purposes; and
- mass of electronic components (flight controller, motor speed controllers, etc.) = 0.3 kg.

In order to estimate the drone mass, the following assumptions have been considered:

- motor mass = 0.1 kg;
- propeller mass = 0.01 kg;
- annular element mass = $3.6\,\text{kg/m}^2 \times \pi \times D^2/4$; and
- battery cell mass = 1.11 kg.

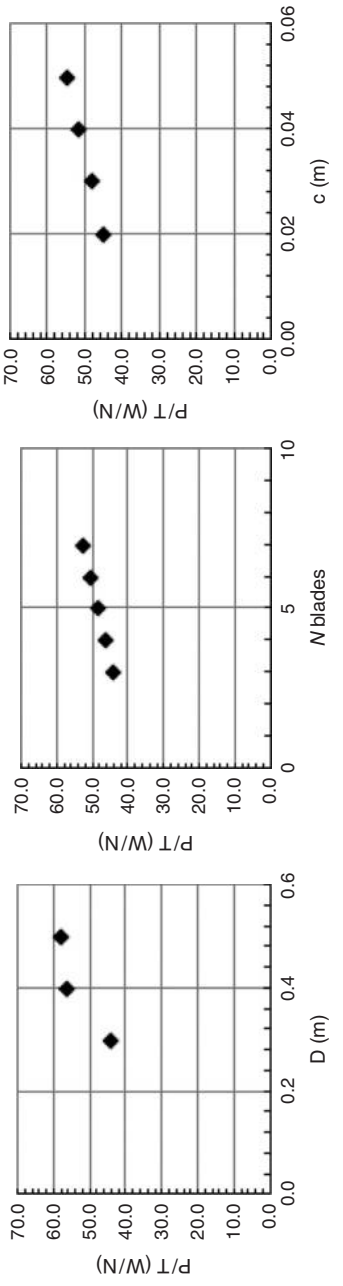

Figure 6.
P/T sensitivity analysis

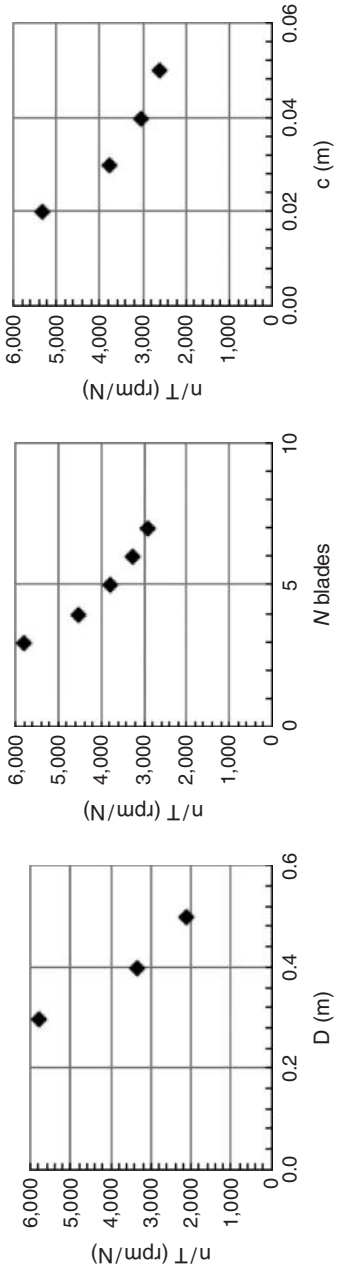

Figure 7.
n/T sensitivity analysis

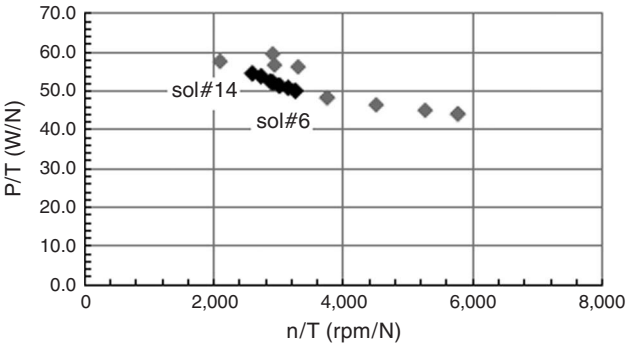

Figure 8.
Summary of propeller performance

Propeller: sol#6	Performance	Propeller: sol#14	Performance
$D = 0.3$ m	$P/T = 50$ W/N	$D = 0.3$ m	$P/T = 55$ W/N
$N = 6$	$n/T = 3{,}257$ rpm/N	$N = 5$	$n/T = 2{,}591$ rpm/N
$\theta = 0$ deg	$T = 3.07$ N	$\theta = 0$ deg	$T = 3.86$ N
$c = 0.03$ m	$P = 154$ W	$c = 0.05$ m	$P = 211$ W
$\lambda = 1$		$\lambda = 1$	
Advantages	Higher flight endurance	Advantages	Lower motor speed required
Disadvantages	Higher motor speed required	Disadvantages	Lower flight endurance

Table II.
Propeller selected solutions

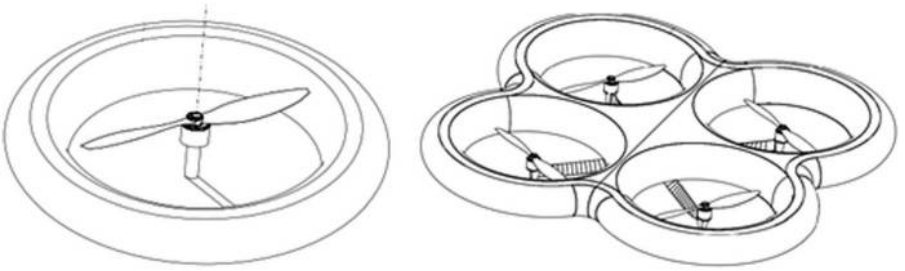

Figure 9.
Drone module (left) and example of quadcopter configuration (right)

Source: Cipolla *et al*. (2015)

Concerning batteries, the SAFT VES180 cells have been considered (Borthomieu and Prévot, December 2005). These Li-ion cells, which have been used in the past on Mars exploration rovers (e.g.: Pathfinder), have been selected for their specific energy, as high as 165 Wh/kg and their compact dimensions (53 mm × 250 mm). Each cell has a mass of 1.11 kg and is able to store up to 180 Wh. Since the mean discharge voltage is 3.6 V (4.1 V at the end of charge) and considering a typical motor voltage of 11 V, three VES180 cells in series are required. Therefore, the assembled battery pack is estimated to have a mass of 3.33 kg. Under these assumptions, four reference drone configurations have been obtained, as illustrated in Table III.

In particular, it is worth noting that:

- the hexacopter 6Xsol#6, shown in Figure 10, has the best endurance performance but the maximum required rotating speed is slightly higher than 11,000 which may affect the cooling capabilities of motors;

No. of rotors	"Hexacopter" 6		"Octocopter" 8	
Propeller configuration	sol#6	sol#14	sol#6	sol#14
Total mass (kg)	6.52	6.52	7.25	7.25
Airframe	1.53	1.53	2.04	2.04
Propellers	0.06	0.06	0.08	0.08
Motors	0.60	0.60	0.80	0.80
Batteries	3.33	3.33	3.33	3.33
Electronics	0.30	0.30	0.30	0.30
Sensors	0.70	0.70	0.70	0.70
Weight on Mars (N)	19.6	19.6	21.7	21.7
Max. required thrust (N)	21.5	21.5	23.9	23.9
Max. required rotating speed (rpm)	11,675	9,286	9,736	7,743
Max. power consumption (W)	1,079	1,175	1,199	1,307
Motors voltage (V)	11	11	11	11
Max. current (A)	16	18	14	15
Flight endurance (min)	31	28	27	25
Airframe diameter (m)	0.96	0.96	1.20	1.20

Table III. Resulting drone reference configurations

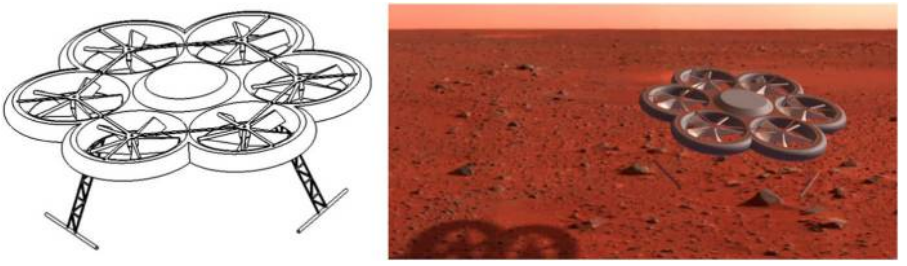

Figure 10. Conceptual layout and artistic view of the 6Xsol#14 configuration

- the octocopter 8Xsol#14 has a low rotating speed but it features also the lowest endurance among the selected configurations;
- solutions 6Xsol#14 and 8Xsol#6 are both suitable and comparable for the application discussed here; and
- solution 6Xsol#14 may be preferred since it has lower mass, smaller airframe dimension and slightly higher endurance.

7. Entry capsule and docking station preliminary design

As shown in Table I, the overall probe payload is estimated to be around 80 kg. Within this mass, the entry probe and the drone itself have to be accommodated. It is well known that the atmospheric entry is one of the main issues of planetary missions, thus the entry capsule has been sized following the already space proven design. In particular, the Beagle 2 entry capsule is considered as reference (Pullan *et al.*, 2004).

The station and the drone are protected during the transfer and the entry by an aeroshell composed of the heat shield and the backshell. The heat shield is assumed to be covered by 8 mm thick TPS ablating during entry, whereas the parachute is assumed to be stowed in the backshell. The landing system is completed by an airbag system which has to be inflated few seconds before touching ground.

Beagle 2 capsule total mass was about 68.5 kg (thus fitting in the spacecraft payload mass estimated) with a payload landed on the surface of about 33.2 kg. The capsule had overall dimensions comparable with the size required to host the drone configurations conceived. In particular, it had a maximum radius of 462 mm, a length of 523 cm and was based on a 60° sphere-cone design with 0.4 m noise radius and a base area of 0.67 (Davies, 2006).

Taking these data as reference, Table IV summarizes the entry capsule/docking station sizing.

Solar array system has been sized scaling the Beagle 2 power generation system (Pullan *et al.*, 2004). An input power of 80 W is made available for the whole surface module, during the charging periods up to 75 percent can be dedicated for charging the drone. The docking station is conceived to deploy eight identical solar panels double folded within the entry capsule maximum diameter. In the center, the docking platform and the telecommunication system are placed. This design reduces also the problem of having the solar panels covered by dust during drone landing/lifting as the Mars surface in the neighborhood of the docking platform is shielded by solar panels.

Data acquired during drone missions are downloaded on the OBC (properly equipped with a solid-state mass memory) and the station uploads these data during the idle periods (drone operations). One battery pack of the same kind as the ones accommodated on the drone is considered for the station. This can be used both to increase the drone charging speed and to face potential power peak periods.

The telecommunication system is conceived to operate in the X band for data uplink and UHF for downlink. The system is also in charge of communicating the docking station status and position to the probe. The beacon, instead, is switched on after the

	Mass		Power budget during entry		Power budget in charging mode		Power budget in transmitting mode	
Subsystem	Kg	% of total	W	% of total	W	% of total	W	% of total
Aeroshell and heat shield	17	25.0	8	10.0	0	0.0	0	0.0
Parachute	3.1	4.6	8	10.0	0	0.0	0	0.0
Airbag	13.6	20.0	4	5.0	0	0.0	0	0.0
Structure (incl. docking system)	11.6	17.1	0	0.0	0	0.0	0	0.0
Position beacon	0.5	0.7	4	5.0	4	5.0	4	5.0
Solar arrays	6.4	9.4	1	1.3	1	1.3	1	1.3
Battery	3.3	4.9	2	2.5	2	2.5	2	2.5
Telecomm. System	2.7	4.0	16	–	2	–	56	–
OBC	2	2.9	10		10		10	
Harness	0.3	0.4	0		0		0	
Total w/o payload	60.5	89.0	53	66.3	19	23.8	73	91.3
Hexacopter								
Drone mass/power	6.5	9.6	0	0.0	60	75.0	0	0.0
System-level margin	1	1.5	27	33.8	1	1.3	7	8.8
Total	68	100.0	80	100.0	80	100.0	80	100.0
Octocopter								
Drone mass/power	7.3	10.7	0	0.0	60	75.0	0	0.0
System-level margin	0.2	0.3	27	33.8	1	1.3	7	8.8
Total	68	100.0	80	100.0	80	100.0	80	100

Table IV.
Entry capsule/ docking station preliminary mass and power budget

capsule deploying (together with the one embedded in the backshell) and works as a reference point for the navigation system of any drone of the fleet. Since this is a single-point failure component for the mission of any drone of the fleet, a cold redundancy can be considered with marginal impact on the capsule mass budget.

OBC, beacon, solar arrays and batteries are assumed to have a constant power consumption/dissipation, whereas the descending equipment is assumed to operate only during the entry scenario. As shown in Table IV, 80 W is sufficient to operate the station and to recharge the drone in all scenarios considered. Due to the power limitation constraints, however, the drone battery charging time is estimated to be around 200 minutes (at 3.6 V).

Once landed, the base plate of the probe is designed to open and expose solar panels and the docking mechanism. The docking mechanism is designed to be robust, by means of a physical mating of drone and docking station surfaces, and the charging mechanism relies on an inductance system. Such a system offers also a safe base for drone's protection during dust storms when operations shall be forbidden.

8. Conclusions

This paper deals with the study of an innovative unmanned mission to Mars, aimed at acquiring a great amount of detailed data of Mars' atmosphere and its surface. The main innovation of the mission proposed consists in the adoption of small multi-copter UAVs, also called "drones," as remote-sensing platforms. Such innovation is made possible thanks to other two enabling technologies: the use of three (or more) small satellites instead of a bigger one and the use of electric propulsion for the interplanetary transfer, to reduce the propellant mass fraction and thus increasing the payload mass.

The mission has been designed by taking a spacecraft size at the limit between small- and medium-class satellites (500 kg) into account and designing the Earth-Mars low-thrust transfer trajectory following a minimum mass approach. As a result, the time estimated for the Earth-Mars transfer is slightly more than 27 months with a propellant amount of about 125 kg, coherent with the choice of considering a 500 kg-class spacecraft.

As shown in Figure 11, almost 25 percent of the whole spacecraft mass budget must be allocated for the propellant required for the Earth-Mars transfer. The two heaviest subsystems are the power generation system and structure and mechanism, whereas the other subsystems have an impact on mass budget by less than 10 percent each. In this configuration up to 16 percent (80 kg) can be allocated for the payload, which consists of the entry capsule used to deliver the drone and its docking/charging station on the Mars surface.

The spacecraft preliminary power budget has been defined and solar arrays have been sized by considering the most power-demanding conditions, i.e. during the final capture phase when the probe is around Mars and the electric propulsion

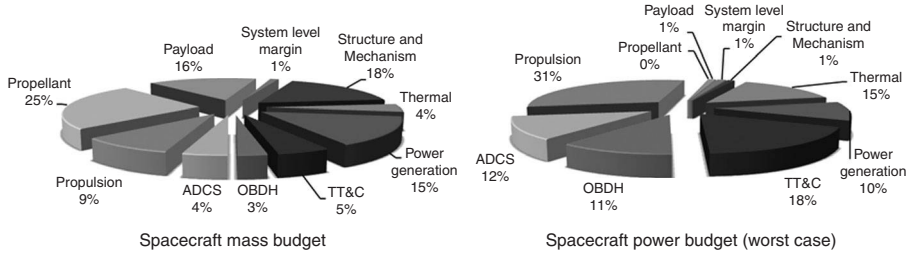

Figure 11. Spacecraft mass (left) and power (right) budget in worst-case scenario (firing mode around Mars)

system is operated. Figure 11 illustrates this worst-case scenario showing that still in this condition 1.3 percent of available power (50 W) is left as the system-level margin. Payload is kept in hibernation mode with minimum power requirement, whereas the other subsystems require from 10 percent (power generation system) to 31 percent (propulsion system).

The drone has been designed by considering at first the problem of operating propellers and brushless motors in the tiny Mars atmosphere, whose density is about 1 percent of the Earth. Ducted propellers have been chosen in order to increase the static thrust, which is the most relevant performance for hovering conditions, and brushless motor characteristics by the literature have been taken into account.

Given a set of requirements, among which 30 minutes of endurance and 0.7 kg of embarked sensors (drone's payload), the propeller design has been carried out by implementing the DFDC approach. A preliminary sensitivity analysis of the main performance parameters identified the *P/T* and the rotating speed-to-thrust ratios as the most fundamental ones. These have been considered as drivers to design a set of design parameters. Among these, duct diameter, mean blade chord and number of blades are the most influential, with contrasting effects on the aforementioned performance parameters. Four compromise potential solutions have been identified and compared, taking also endurance, mass and size into account. The baseline solution identified is characterized by six rotors, a total mass of about 6.5 kg and a flight endurance of 28 minutes.

Finally, the preliminary design of the entry capsule (designed to operate also as a docking station and data relay system) has been faced, providing mass and power breakdown and verifying the capability of hosting the selected drone configuration. As shown in Figure 12, 68 kg of the entry capsule/docking station is mainly devoted for the atmospheric entry and landing devices: aeroshell and heat shield, airbag and parachute compose 50 percent of the whole mass. Two capsule configurations have been sized, the first one designed for a hexacopter drone and the second one for a octocopter, and even in the worst-case condition (the octocopter has a mass of 1.2 kg more than the hexacopter) a system-level margin of 0.2 kg is left.

From the power budget point of view, the worst case, shown in Figure 12, is the charging mode, in which the drone is docked and requires 75 percent of the power generated by the docking station. In this condition, which has been taken into account to size the batteries of the entry capsule/docking station, a system-level margin of 1.3 percent is still guaranteed. In such operating mode the second most power-demanding subsystem is the position beacon, which must be working continuously since it acts as a reference point for the entire drone fleet.

As a general conclusion, the study shows the mission concept feasibility. The concept would return incomparable scientific data and can be also potentially

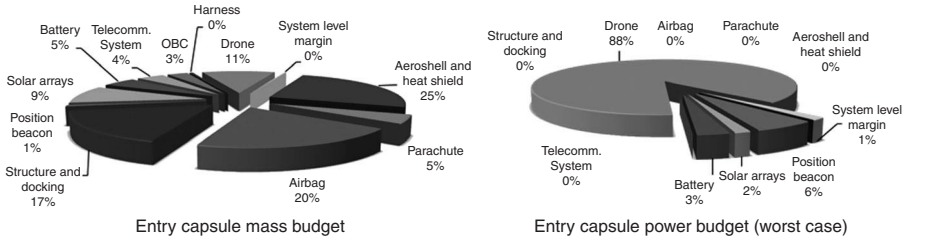

Figure 12.
Entry capsule/docking station mass (left) and power (right) budget in worst-case scenario

implemented with a relatively low budget exploiting of the shelf components to a larger extent, small identical spacecraft buses and modular low-cost drones.

Further research topics will deal with the refinement of the low-thrust mission analysis, taking the actual working point of the electric thruster considered into account and the trajectory optimization will be improved by using ephemeris and a full force model. Concerning the drone design, an optimization of propeller aerodynamics by means of computational fluid dynamics analyses will be carried out, aiming to assess more in detail the propulsion performance and to check the proper cooling of BLDC motors. A more accurate sizing of all the subsystems of both the spacecraft and the entry capsule will be faced in future studies, changing the power and mass budget specific figures, but without affecting the overall mission design.

References

Albee, A.L., Arvidson, R.E., Palluconi, F.D. and Thorpe, T.E. (2001), "Overview of the Mars global surveyor mission", *Journal of Geophysical Research*, Vol. 106 No. E10, pp. 23291-23316.

Borthomieu, Y. and Prévot, D. (2005), "SAFT VES180 high specific energy cell qualification", Saft Defense and Space Division, Nasa Battery Workshop, Huntsville, December.

Braun, R.D. and Spencer, D.A. (2006), "Design of the ARES Mars airplane and mission architecture", *Journal of Spacecraft and Rockets*, Vol. 43 No. 5, pp. 1026-1034.

Brophy, J.R., Kakuda, R.Y., Polk, J.E., Anderson, J.R., Marcucci, M.G., Brinza, D., Henry, M.D., Fujii, K.K., Mantha, K.R., Stocky, J.F., Sovey, J., Patterson, M., Rawlin, V., Hamley, J., Bond, T., Christensen, J., Cardwell, H., Benson, G., Gallagher, J., Matranga, M. and Bushway, D. (2000), "Ion propulsion system (NSTAR), DS1 technology validation report", JPL Publication 00-10, 10/2000, NASA/JPL, Pasadena, CA.

Bryson, A.E. and Ho, Y.C. (1975), *Applied Optimal Control*, Hemisphere Publishing Corporation, Washington, DC.

Cipolla, V., Frediani, A., Lonigro, E., Oliviero, F. and Rizzo, E. (2015), "Struttura di drone ad elevata efficienza aerodinamica" (transl. "Drone structure with high aerodynamic efficiency"), Italian Patent Office request n.UB2015A003894, Pisa.

Clapp, W.M. (1984), "Dirigible airships for martian surface exploration", *The Case for Mars II*, Vol. 62, American Astronautical Society Science and Technology Series, pp. 489-496.

Davies, C. (2006), "Planetary mission entry vehicles: quick reference guide, Space Technology Division", Version 3, NASA/SP-2006-3401, NASA Ames Research Center, CA.

Deep Space 1 Press Kit (1998), JPL, October, 10-1-98-JPL, NASA HQ historical reference collection.

Development Sciences Incorporated (1978), "A concept study of a remotely piloted vehicle for Mars exploration", NASA CR-157942, Development Sciences Incorporated, City of Industry, CA.

Drela, M. and Youngren, H. (2005), "Axisymmetric analysis and design of ducted rotors", theory document, DFDC, MIT, Cambridge, MA.

Edquist, K.T., Desai, P.N. and Schoenenberger, M. (2008), "Aerodynamics for the Mars phoenix entry capsule", *AIAA/AAS Astrodynamics Specialist Conference and Exhibit, AIAA, Honolulu, August*, pp. 2008-7219.

Girones-Lopez, J., Schmanke, D., Klingelhoefer, G., Maul, J., Brueckner, J., Duston, C., Gellert, R. and Klingelhöfer, G. (2010), "The alpha particle X-ray spectrometer APXS on the Rosetta lander Philae to explore the surface of comet 67P/Churyumov-Gerasimenko", 38th COSPAR Scientific Assembly, Bremen, July.

Goebel, G. (2010), "The NASA ERAST HALE UAV Program", Unmanned Aerial Vehicles.

Guest, J.E., Butterworth, P.S. and Greeley, R. (1977), "Geological observations in the Cydonia region of Mars from viking", *Journal of Geophysical Research*, Vol. 82 No. 28, pp. 4111-4120.

Hall, D.W. and Parks, R.W. (1998), "On the development of airborne science platforms for martian exploration", *Proceedings of the Founding Convention of the Mars Society, Univelt*, San Diego, CA, p. 323.

Helmbold, H.B. (1955), "Range of application of shrouded propellers", School of Engineering, University of Wichita, Wichita, KS.

Justus, C.G., Duvall, A. and Johnson, D.L., "Mars global reference atmospheric model (MARS-GRAM) and database for mission design", Marshall Space Flight Center.

Kuchemann, D. and Weber, J. (1953), *Aerodynamics of Propulsion*, McGraw-Hill, London.

Law, D.C., Edmondson, K.M., Siddiqi, N., Paredes, A., King, R.R., Glenn, G., Labios, E., Haddad, M.H., Isshiki, T.D. and Karam, N.H. (2006), "Lightweight, flexible, high-efficiency III-V multijunction solar cells", *Proceedings of the IEEE 4th World Conference on Photovoltaic Energy Conversion, Waikoloa, HI, May*, pp. 1879-1882.

Lutz, T., Gu, C., Gardecki, S., Cordes, F. *et al.* (2014), "Startiger dropter project: development and flight experiment of a skycrane-like terrestrial lander demonstrator", *Proceedings of the ESA GNC 2014: 9th International ESA Conference on Guidance, Navigation and Control Systems (GNC-2014), June 2, Porto*.

McCleese, D.J., "Robotic Mars exploration strategy 2007-2016", Mars Advanced Planning Group, JPL 400-1276 7/06.

Maimone, M.W., Johnson, A.E., Cheng, Y., Willson, R.G. and Matthies, L. (2006), "Autonomous navigation results from the Mars exploration rover (MER) mission", *Springer Tracts in Advanced Robotics*, Vol. 21 No. 1, pp. 3-13.

Malla, R. (2000), "Martian airborne exploration vehicle", Wichita State University, Department of Aerospace Engineering, HEDS-UP Forum, Wichita, KS, May.

Mars Odyssey Arrival Press Kit (2001), JPL, October, 10-16-01-JPL, NASA HQ historical reference collection.

New Horizons Launch Press Kit (2006), JPL, January, APL-2006a, NASA HQ historical reference collection.

Phillips, R., Palladino, M. and Courtois, C. (2012), "Development of brushed and brushless DC motors for use in the Exomars drilling and sampling mechanism", 41st Aerospace Mechanisms Symposium, Jet Propulsion Laboratory, Pasadena, CA, May.

Pullan, D., Sims, M.R., Wright, I.P., Pillinger, C.T. *et al.* (2004), "Beagle 2: the exobiological lander of Mars express", European Space Agency (special publication) ESA SP-1240.

Rover Environmental Monitoring Station. Centro de Astrobiología (CSIC-INTA), available at: http://cab.inta-csic.es/rems/en

Sovey, J.S., Rawlin, V.K. and Patterson, M.J. (2001), "Ion propulsion development projects in US: space electric rocket test 1 to deep space 1", *Journal of Propulsion and Power*, Vol. 17 No. 3.

Wertz, J.R., Everett, D.F. and Puschell, J.J. (2011), *Space Mission Engineering: The New SMAD*, Microcosm Press, Hawthorne, CA.

Corresponding author
Vittorio Cipolla can be contacted at: vittorio.cipolla@for.unipi.it